A Model for Partial Viscous Sintering

Ming-shen M. Sun, J. Christian Nelson, Joseph J. Beaman, Joel J. Barlow
The University of Texas at Austin

Abstract

A mathematical model describing the sintering rate of a viscous material powder bed is presented. This model assumes that the powder bed is composed of cubic packed, equal-size spherical particles. The sintering rate equation is derived in terms of a unit cell dimension or the relative density of a powder bed. A mathematical factor, fraction of sintering, is introduced to explain the phenomena of partial sintering. *Key words: model, viscous sintering.*

I. Introduction

The theory of viscous sintering was first explored by Frenkel [1]. The primary concept of his theory is: energy balance between the work done by surface tension (the surface energy loss) and viscous dissipation during the particle deformation. Frenkel's model was derived to explain the sintering behavior of two spherical particles and it was proven to be valid only in the initial stage of sintering [2]. Extending Frenkel's concept, Scherer [3-5] has developed a cylinder structure model that can successfully describe sintering behavior of a viscous glass preform. However, for some applications that apply the sintering of a randomly packed viscous powder bed such as the Selective Laser Sintering [6], Scherer's model does not give a correct geometric description of the powder bed, and it can not explain the observed sintered depth and temperature dependency of steady state density. A new model of powder bed sintering, also based on Frenkel's concept is presented in this paper. This model assumes a cubic packed powder bed structure. By introducing a mathematical factor, fraction of sintering, this model can explain the temperature dependency behavior of sintered bed density. The effect of variation in particle size can also be considered in calculating the sintering rate.

II. Structure of the Powder Bed

In some of applications employing sintering of powder beds such as the Selective Laser Sintering, the powder bed is a structure of randomly packed spherical particles as shown in figure 1. A cubic packed structure is a powder bed composed of equal-size spherical particles alined in a cubic way (figure 2). The measured relative density (solid fraction) values of several Selective Laser Sintering powders and the calculated relative density of the cubic packed structure are listed in Table 1. It is found that the relative density of a randomly packed powder bed is not far from the relative density of a cubic packed structure, therefore we choose the cubic packed structure to represent the structure of a randomly packed powder bed. The advantage of using the cubic packed structure is its geometric simplicity. It is also assumed that the powder bed remains in cubic packed structure during the sintering process. Sintering rate equations derived hereafter are all based on this geometric assumption. Although for other types of powder bed packing,

46

similar sintering rate equations can be derived using the same concept. The cubic packed structure will give the simplest mathematic form.
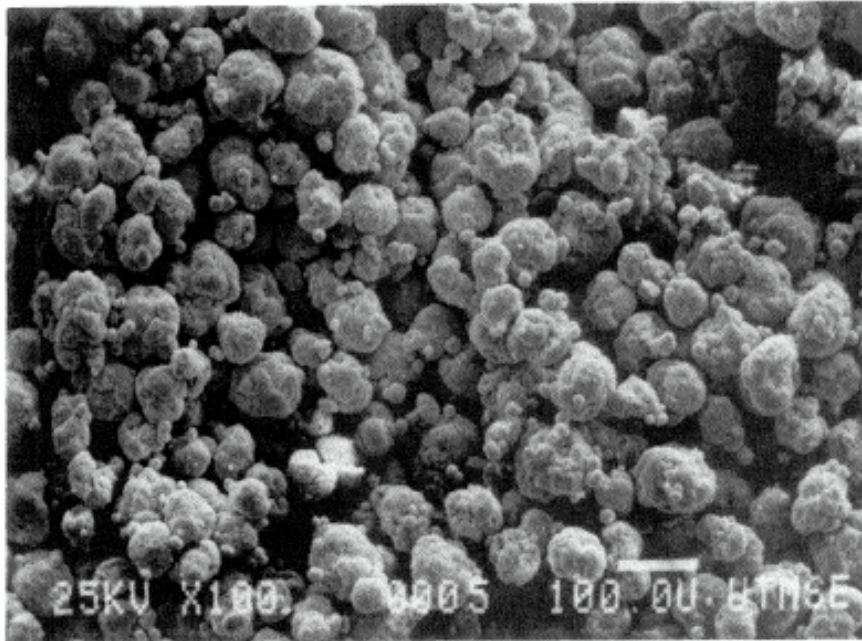

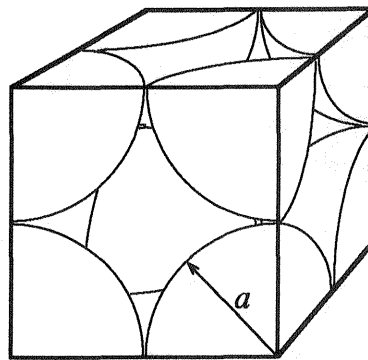
Figure 1. A randomly packed PVC powder bed.

Figure 2. The cubic packed structure

Table 1. The relative density of some Selective Laser Sintering powders and the cubic packed bed

Powder	Particle Shape	Avg. Particle Size	Relative Density
ABS	irregular	120 µm	0.40-0.60
PVC	near spherical	40 µm	0.42-0.50
Polycarbonate	near spherical	50 µm	0.46-0.51
Tin	spherical	70 µm	0.58
Cubic Packed Bed	spherical	any size	0.5236

III. The Sintering Model

Geometrically, the cubic packed structure is a combination of numerous elementary unit cells as in figure 3, each unit cell is a cube in space containing one spherical particle. The length of the cube side is $2x$, which is also the center to center distance between two adjacent particles. It is assumed that during the densification process, each particle within the cell remains primarily a sphere of radius r, and the contact area between two adjacent particles is a circle of radius $\sqrt{r^2-x^2}$. The values of x and r both start equal to a (the initial radius of the particle), x decreases and r increases as the structure densifies. This densification process is illustrated in figure 3.
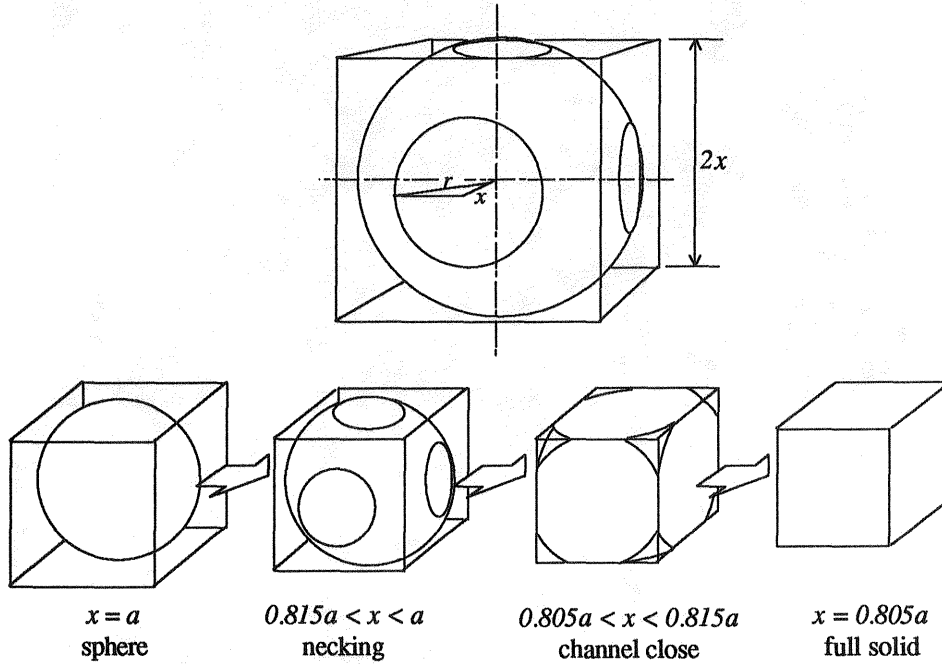

$x = a$	$0.815a < x < a$	$0.805a < x < 0.815a$	$x = 0.805a$
sphere	necking	channel close	full solid

Figure 3. The unit cell and the densification process of a cubic pack structure.

During the densification process, x and r satisfy the volume conservation equation,

$$3x^3 - 9r^2x + 4r^3 + 2a^3 = 0 \tag{1}$$

A critical point in the densification process is when $r=\sqrt{2}x$, where the flat circular area on each side of the cell connect, in other words the channels connecting the void space between the particles close, and the voids are separated. The value of x at this point is $0.8156a$.

After x becomes less than $0.8156a$, the isolated void keeps decreasing in its size until $x=0.805a$ at which time the void vanishes and the structure becomes full solid. The volume conservation equation (1) does not hold in this period since the contact area between two particle is not an exact circle.

However, in most of our sintering experiments of polymer powder, the sintering process ends at a density value which corresponds to an x value larger than $0.8156a$, in other word, most sintering processes end before the pores are separated. Therefore it is reasonable for us to derive the sintering rate equation only for the range $0.8156a<x<a$ where the geometry is simple and the volume conservation equation (1) holds.

By Frenkel's theory, the driving force of sintering is the surface tension of the sintering material, i.e., by decreasing the total surface area of the powder bed structure the

surface energy will reach its minimum. If we assume that sintering occurs between all contacted particle, then the surface area will be a monotonic decreasing function of relative density, and as the powder densifies, the only nontransient resistance force to the surface tension force is the pressure in the pore when the pore channels close and the air is trapped in the pores. Mackenzie and Shuttleworth[9] have established a model describing the densification behavior of porous material containing isolated spherical pores. However, the experimental data shows that most sintering stops even before the pore channels close, therefore, there must be some portion of particles that do not sinter with the others, and as the powder densifies, the surface area of these particles increases, and the surface tension acts also as a resistance force of densification.

For a sintered particle, the contact area vanishes, and the remained surface area of the deformed particle in a unit cell is

$$A_s = 12\pi rx - 8\pi r^2, \tag{2}$$

where x and r satisfy equation (1). A_s is a monotonic decreasing function of r, which means that the surface area decreases as the powder densifies and the surface tension acts as a driving force of densification.

For an unsintered particle, the contact area remains as a boundary between particles, and the surface area of the deformed particle is

$$A_u = 12\pi rx - 2\pi r^2 - 6\pi x^2. \tag{3}$$

This value increases monotonically with r, which means that the surface area increase as the powder densifies. This behavior is mathematically evident because the sphere is the shape of minimum surface area for a given volume. In this case, surface tension acts as a resistant force of densification.

Here we define a factor, fraction of sintering ζ, as the fraction of sintered particles. ζ has a value between 0 and 1. $\zeta=0$ implies no sintering occurs between particles, and $\zeta=1$ implies all particles are sintered together.

Using the factor ζ, the effective surface area of a partially sintered particle is

$$A = \zeta A_s + (1-\zeta)A_u \tag{4}$$

$$= 12\pi rx - (6\zeta+2)\pi r^2 - 6(1-\zeta)\pi x^2 \tag{5}$$

The relationship between A and x given a ζ values can be calculated by solving (1) and (5). The A(normalized by its initial value) x(normalized by a) curves for various ζ values are plotted in figure 4. From these curves, we found that for ζ value less than about 0.3, the surface area initially decreases then increases as powder bed densifies, at the point where the slope of the curve is zero, the surface area rate is zero, and there is no driving force for sintering, which means sintering stops at this point. For the $\zeta=0$ curve, the slope is initially zero, which means that there is no driving force for sintering at the begining, and there will be no spontaneous sintering.
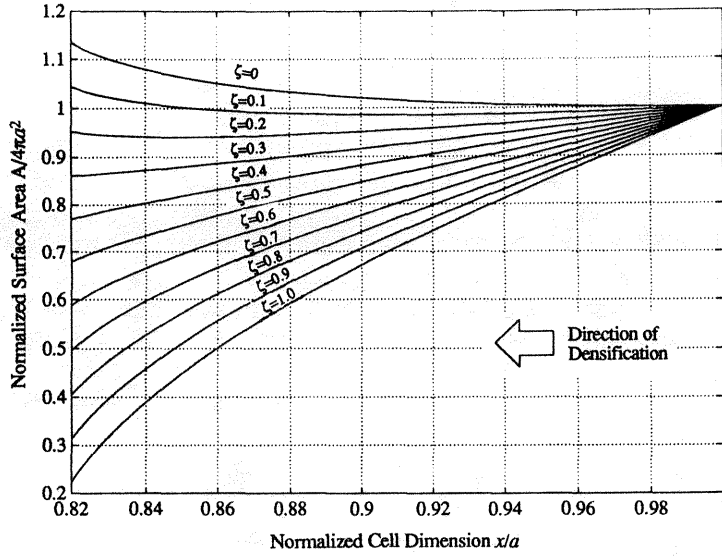
Figure 4. The surface area during densification process

III. The Sintering Rate Equation

From Frenkel's concept, the sintering rate equation is derived from the energy balance equation that the surface energy reduction rate is equal to the viscous dissipation rate during the deformation. For each unit cell, this equation is

$$\gamma \dot{A} + \eta_b \dot{\epsilon}^2 V = 0 \tag{6}$$

where γ (N/m) is the surface tension of the material. η_b (Pa·sec) is the bulk viscosity of the porous structure, $\dot{\epsilon}$ is the volumetric strain rate of the structure and V(m^3) is the volume of the unit cell.

The surface area rate $\dot{A}$ can be derived from (5) as

$$\dot{A} = 12\pi(\dot{r}x + r\dot{x}) - 2(6\zeta + 2)\pi r\dot{r} - 12(1 - \zeta)\pi x\dot{x}, \tag{7}$$

where x and r satisfy equation (1), and $\dot{x}$ and $\dot{r}$ satisfy the derivative of equation (1):

$$9x^2\dot{x} - 18rx\dot{r} - 9r^2\dot{x} + 12r^2\dot{r} = 0 \tag{8}$$

In equation (6), the bulk viscosity η_b is a function of the true viscosity of the material and the relative density, various models have been proposed to describe their relations [7-8]. Skorohod's model [8] which directly relate η_b to the relative density ρ is used here,

$$\eta_b = \frac{4\eta\rho^3}{3(1-\rho)}, \tag{9}$$

where η is the viscosity of the liquid material, and the relative density can be calculated from the geometry of a unit cell as

50

$$\rho = \frac{\pi a^3}{6x^3} \, . \tag{10}$$

Also in (6), the volumetric strain of the unit cell is by definition

$$\varepsilon = 3(1 - \frac{x}{a}), \tag{11}$$

which gives the volumetric strain rate as

$$\dot{\varepsilon} = -\frac{3\dot{x}}{a} \, . \tag{12}$$

The last variable in equation (6) is the volume of the unit cell:

$$V = 8x^3 \tag{13}$$

Substituting (7) to (13) into (6), the final sintering rate equation can be derived as

$$\dot{x} = -\frac{\pi \gamma a^2}{6\eta_b x^3} \left\{ r - (1-\zeta)x + \left[x - (\zeta + \frac{1}{3})r \right] \frac{9(x^2 - r^2)}{18rx - 12r^2} \right\} \tag{14}$$

Integrating equation (14) using standard numerical techniques, the densification curve $x(t)$ or $\rho(t)$ can be obtained. The relation of x/a and ρ versus the normalized time $\pi \gamma t / 6\eta a$ is plotted in Figure 5 with ζ value between 0.1 and 1. These curve are plotted within the range of $0.8156a < x < a$ since the model is derived only for this range.
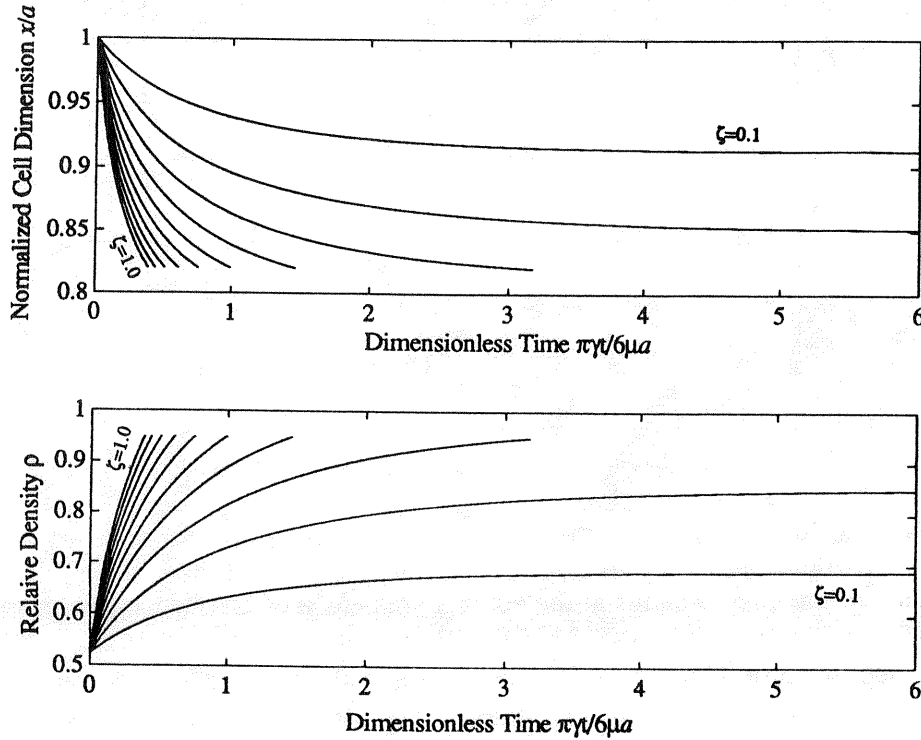

Figure 5. The densification curves

The densification rate increase with increasing γ or ζ, and decreases with increasing η or a. This means that the powder will densify faster with a higher surface tension material, a higher fraction of sintering, a lower viscosity material, or a powder with smaller particle size. Also for ζ value less than about 0.3, the densification process stops before x reaches $0.8156a$ or before the pore channels close. This may explain the observed behavior of lack of pressure sensitivity on final sintered density described elsewhere in this proceedings [9].

IV. Physical Significance of the Factor ζ

For ζ less than about 0.3, the steady state value of x can be determined from the sintering rate equation by seting the sintering rate in equation (14) to zero:

$$r - (1-\zeta)x + \left[x - (\zeta + \frac{1}{3}) \ r \right] \frac{9(x^2-r^2)}{18rx-12r^2} = 0 \qquad (15)$$

The plateau x and ρ values satisfying eq.(15) and eq.(1) can be solved and are plotted in figure 6.
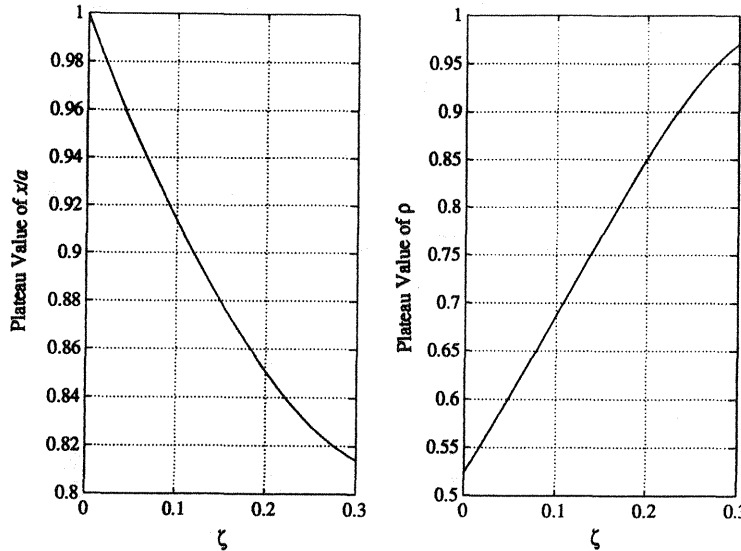
Figure 6. The relation between ζ and plateau values of x/a and ρ.

A physical interpretation of the factor ζ is the probability for forming sintering necks between particles. From a statistical thermodynamic point of view, this probability is directly related to the energy status at the contact area. As a consequence, the probability should increase with temperature because the surface will be at a higher energy state. Also the strain caused by deformation near the contact area will also increase ζ. Strong evidence of the temperature effect on the steady state relative density values is observed in the homogeneous sintering experiment of polymer powder [10]. Shown in figure 7 are some

densification curves of polycarbonate powder at different temperatures. Although the plateau values of the experimental H/Ho curves do not fit the theoretical x/a values in the $\zeta<0.3$ range, the temperature effect is evidenced by the relative plateau values. Possible reasons for the difference between the experimental and theoretical values may include squeeze flow, anisotropic sintering and expansion of gases in the experimental work.
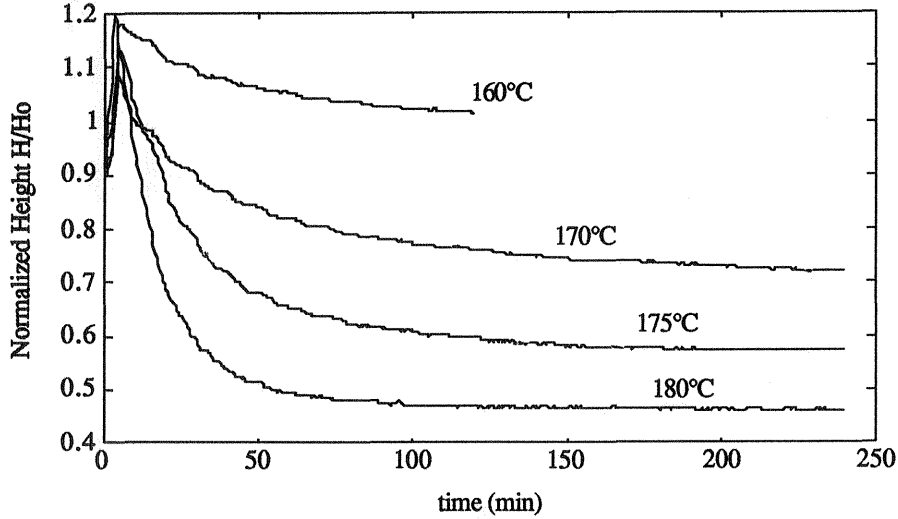

Figure 7. Experimental sintering curves of a polycarbonate powder bed
at different sintering temperature

V. The Effect of Particle Size Distribution

If the particle size of the powder is not uniform but has a variation, the sintering behavior of these particles becomes very complicated and a suitable geometric packing model may not be available. However, if we assumed that the deformation of every unit cell containing one particle is independent from others, the apparent densification behavior can be calculated by volumetrically summing up the deformation curve of each particle.

Assuming that the powder is composed of n_i particles of radius a_i, i=1,2,3.... For every radius, a densification curve $\rho_i(t)$ can be calculated from the sintering rate equation (14). The total volume of the powder bed can be summed up by:

$$V_t = \frac{4\pi}{3}\sum\left(\frac{n_i a_i^3}{\rho_i}\right) = \frac{4\pi}{3}\frac{\sum n_i a_i^3}{\rho} \qquad (16)$$

And the apparent relative density of the powder bed can be calculated by:

$$\rho = \frac{1}{\sum(v_i/\rho_i)} \qquad (17)$$

where $v_i = n_i a_i^3/\Sigma n_i a_i^3$ is the volume fraction for the particle a_i in the powder.

53

The calculated deformation curves of two powder with different particle size distribution are shown in figure 8. Form this curve, we can see that powder with smaller particles will have higher densification rates.
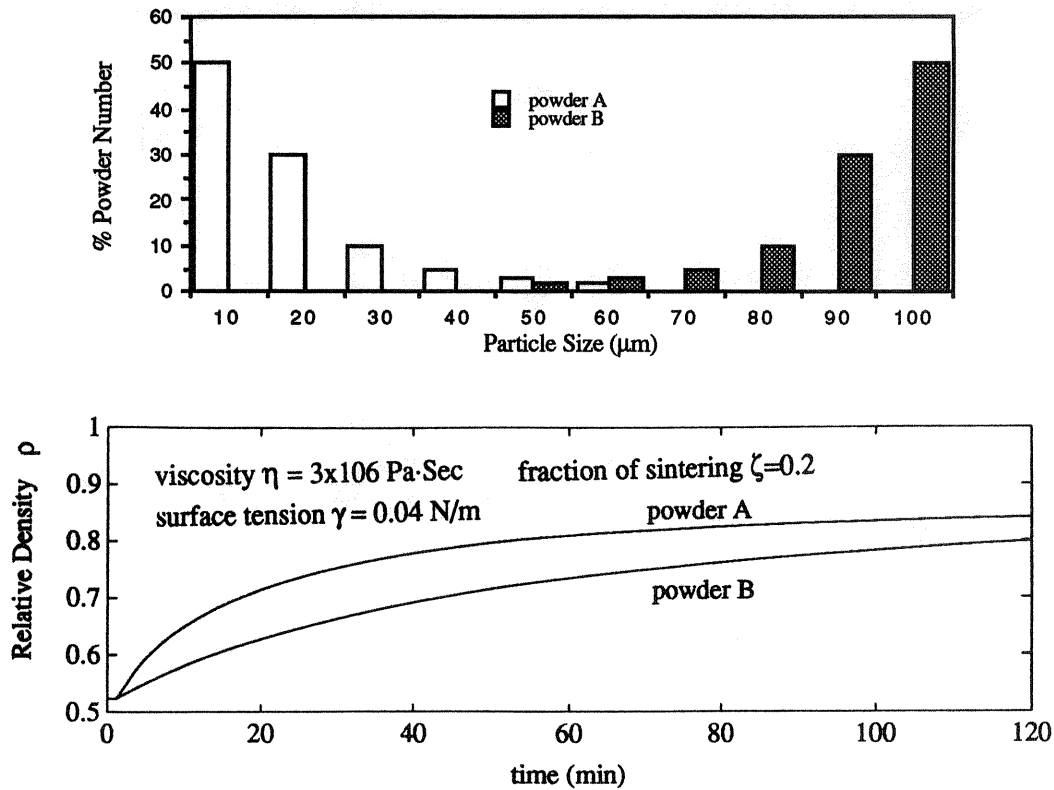

Figure 8. The particle size distribution and densification curve of two powders

VI. Summary

A model is presented which estimates the sintering in a powder bed of viscous material. This model assumes a cubic packed powder bed structure. A sintering fraction factor ζ is introduced to this model to explained the partial sintering behavior observed in most sintering experiments which other sintering models do not consider. A sintering rate equation is derived based on the energy balance equation. The calculated densification curves qualitatively depict the characteristics of a real sintering process. Incomplete sintering is approximated by sintering curves with ζ value less than about 0.3. A physical interpretation of the ζ factor and it's relation with temperature is discussed. Finally, the model is augmented with a particle size distribution effect.

References

1. Frenkel, J., *"Viscous Flow of Crystalline Bodies Under the Action of Surface Tension,"* J. Phys. (Moscow), **9** [5] 385-91 (1945).
2. Rosenzweig, N., Narkis, M., *"Dimensional Variations of Two Spherical Polymeric Particles During Sintering"*, Pol. Engr. Sci. **21** [10] 582-5 (1981).

3. Scherer, G., *"Sintering of Low-Density Glasses: I, Theory,"* J. Am. Cer. Soc. **60** [5-6] 236-9 (1977).
4. Scherer, G., *"Sintering of Low-Density Glasses: II, Experimental Study,"* J. Am. Cer. Soc. **60** [5-6] 239-45 (1977).
5. Scherer, G., *"Sintering of Low-Density Glasses: III, Effect of a Distribution of Pore Size,"* J. Am. Cer. Soc. **60** [5-6] 245-8 (1977).
6. Dekard, C., *"Selective Laser Sintering,"* PhD. Dissertation, The University of Texas at Austin (1988).
7. Bordia, R., Scherer, G., *"On Constrained Sinteing-I. Constitutive Model for a Sintering Body,"* Acta matall. **36** [9] 2393-7 (1988).
8. Bordia, R., Scherer, G., *"On Constrained Sinteing-II. Comparison of Constitutive Models,"* Acta matall. **36** [9] 2399-409 (1988).
9. Nelson, J. C., Vail, N. K., Barlow, J. W., *"Post-Processing of Selective Laser Sintered Polycarbonate Parts,"* SFF Symposium, Austin, TX (1991).
10. Nelson, C., Barlow, J., *"Sintering Rates in the Selective Laser Sintering,"* SFF Symposium, 164-70, Austin, TX (1990).